Sliding Mode Control of Anti-lock Braking System based on Reaching Law Method

Darko Mitić[1], Dragan Antić[2], Staniša Perić[3], Marko Milojković[4] and Saša Nikolić[5]

Abstract – **To improve the performances of anti-lock braking system, sliding mode control with constant plus proportional reaching law method is discussed in this paper. The proposed approach is verified through digital simulation and experimental results showing good system characteristics.**

Keywords – **Antilock braking system, Wheel slip, Sliding mode control, Reaching law method.**

I. INTRODUCTION

In order to prevent the wheels to stop completely during a sudden braking, an anti-lock braking system (ABS) is used as a standard equipment in modern vehicles. In the absence of ABS, during the braking phase, when the wheels are completely locked, the control over vehicle could be lost and it can skid in an undesirable direction. ABS does not allow the wheels to be stiffened and thus enable driver to normally operate with the vehicle.

The main objective of the ABS controller is to ensure the best adhesion of a wheel to a surface. This is performed by controlling the road adhesion coefficient representing the proportion between the friction force, generated during the acceleration and braking phase, and the normal load of the vehicle. It is shown that this coefficient is in nonlinear dependence on the wheel slip, defined as the relative speed difference between the wheel and vehicle. ABS controller is usually designed to regulate the wheel slip so that the road adhesion coefficient has a maximum value. The optimal value of wheel slip should be in the range from 0.08 to 0.3 [1].

ABS is a nonlinear system whose nonlinearities are reflected in unknown parameters of vehicle environment and nonlinear characteristics of braking dynamics. Besides that, the system parameters vary, which is caused by components deterioration, and many external disturbances cannot be predicted in advance. That is why sliding mode control (SMC) methods seem to be the right choice in the control of ABS.

SMC belongs to the well-studied class of discontinuous nonlinear control systems [2-4]. Sliding mode is of particular interest in these systems and it occurs when the system state is forced to move along a predefined sliding surface, determined by the so-called switching function. The switching function dynamics can be defined by using the so-called reaching law method [3]. The constant plus proportional variant of this control approach is used in this paper. If sliding mode exists, a system becomes robust to parameter variations and external disturbances, and its dynamics is known in advance and usually of the low order. The shortcoming of SMC is the existence of the chattering phenomenon. It occurs as the consequence of the high frequency control signal, which can excite the system's unmodelled dynamics.

[1,2,3,4,5]All authors are with the University of Niš, Faculty of Electronic Engineering, A. Medvedeva 14, 18000 Niš, Serbia, E-mail:{darko.mitic, dragan.antic, stanisa.peric, marko.milojkovic, sasa.s.nikolic}@elfak.ni.ac.rs.

Traditional SMC enhanced by a grey system theory is proposed in [5, 6]. Digital simulation results of ABS with conventional SMC, where hydraulic brake dynamics is neglected during the design, is shown in [7]. The combination of SMC and the sliding mode observer is elaborated in [8]. In [9], the SMC, allowing the maximum value of the wheel–road friction force during the braking phase, without *a priori* knowledge of optimal slip, is discussed. The adaptive SMC of vehicle traction is considered in [10]. The integration of SMC and pulse width modulation (PWM) method, realized by using computer software as opposed to hardware, is given in [11, 12]. For overall vehicle stability enhancement, the traditional SMC is also used in wheel slip control [13].

II. ANTI-LOCK BRAKING SYSTEM MODEL

We consider the system shown in Fig. 1 [14] with two rolling wheels: the lower car-road wheel and the upper car wheel which is in a rolling contact with the lower wheel. Two optical encoders are installed on both of the wheels to measure the angles with the resolution of $2\pi/2048 = 0.175°$. The wheel angular velocities are not measured and they are estimated by Euler formula with the sample time period of 0.5 ms.

The upper wheel is equipped in the disk brake system driven by the small *DC* motor. The lower wheel is coupled to the big flat *DC* motor using to accelerate the wheel and its power supply is switched off during the braking phase. Both *DC* motors are controlled by 3.5 kHz pulse-width modulation (PWM) signals.

The Fig. 1 shows the simple quarter vehicle model treating only longitudinal motion of the vehicle and angular motion of the wheel, while the lateral and the vertical motions are neglected. There is no influence of other vehicle wheels.

The car velocity is equal to the angular velocity of the lower wheel multiplied by the radius of this wheel, while the angular velocity of the wheel is equal to the upper wheel angular velocity. According to Fig. 1, x_1 represents the angular velocity of the upper wheel, x_2 is the angular velocity of the lower wheel and r_1, r_2 represents the radius of the upper and lower wheel, respectively.

A braking torque is applied to the upper wheel during braking phase causing wheel speed to decrease. Introducing the auxiliary variables:

$$s = \operatorname{sgn}\left(r_2 x_2 - r_1 x_1\right),\ s_1 = \operatorname{sgn}\left(x_1\right),\ s_2 = \operatorname{sgn}\left(x_2\right). \tag{1}$$

The equation of the upper wheel motion is given in the following form:

$$J_1\dot{x}_1 = F_n r_1 s\mu\left(\lambda\right) - d_1 x_1 - s_1 M_{10} - s_1 M_1\,, \tag{2}$$

by using the Newton's second law, where: J_1 is the moment of inertia, d_1 is the viscous friction coefficient and M_{10} is the static friction of the upper wheel. According to (2), the friction force is assumed to be proportional to the normal pressing force F_n, where $\mu(\lambda)$ is the coefficient of proportion called the road adhesion coefficient.

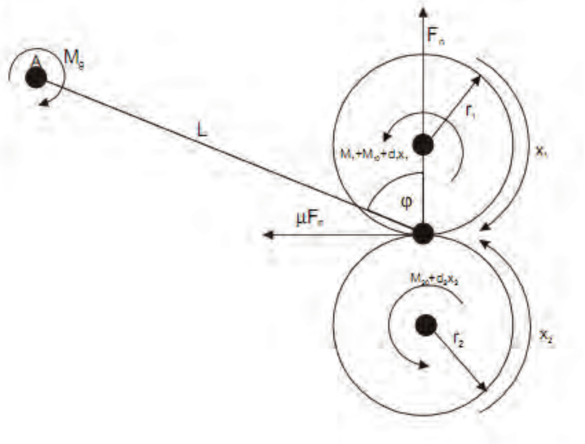

Fig. 1. ABS model (graphical presentation)

The lower wheel motion can be described by:

$$J_2\dot{x}_2 = -F_n r_2 s\mu\left(\lambda\right) - d_2 x_2 - s_2 M_{20}\,, \tag{3}$$

where J_2 is the moment of inertia, d_2 is the viscous friction coefficient and M_{20} is the static friction of the lower wheel. To derive the normal force F_n, we write the sum of torques corresponding to the point A in Fig. 1 as:

$$F_n L\left(\sin\varphi - s\mu\left(\lambda\right)\cos\varphi\right) = M_g + s_1 M_1 + s_1 M_{10} + d_1 x_1\,, \tag{4}$$

yielding:

$$F_n = \frac{M_g + s_1 M_1 + s_1 M_{10} + d_1 x_1}{L\left(\sin\varphi - s\mu\left(\lambda\right)\cos\varphi\right)}\,, \tag{5}$$

where M_g represents gravitational and shock absorber torques acting on the balance lever, L is the distance between the contact point of the wheels and the rotational axis of the balance and φ is the angle between the normal in the contact point and the line L.

Replacing F_n from (5) in (2) and (3), the model becomes:

$$J_1\dot{x}_1 = \frac{M_g + s_1 M_1 + s_1 M_{10} + d_1 x_1}{L\left(\sin\varphi - s\mu\left(\lambda\right)\cos\varphi\right)} r_1 s\mu\left(\lambda\right) - s_1 M_1 - d_1 x_1 - s_1 M_{10}\,,$$

$$J_2\dot{x}_2 = -\frac{M_g + s_1 M_1 + s_1 M_{10} + d_1 x_1}{L\left(\sin\varphi - s\mu\left(\lambda\right)\cos\varphi\right)} r_2 s\mu\left(\lambda\right) - d_2 x_2 - s_2 M_{20}\,. \tag{6}$$

While the wheel angular velocity would match the forward car velocity in the normal operating conditions, in the course of the braking and the acceleration phases these velocities differs one from other. Their difference is called a wheel slip λ, defined as:

$$\lambda = \begin{cases} \dfrac{r_2 x_2 - r_1 x_1}{r_2 x_2}, r_2 x_2 \ge r_1 x_1, x_1 \ge 0, x_2 \ge 0, \\ \dfrac{r_1 x_1 - r_2 x_2}{r_1 x_1}, r_2 x_2 < r_1 x_1, x_1 \ge 0, x_2 \ge 0, \\ \dfrac{r_2 x_2 - r_1 x_1}{r_2 x_2}, r_2 x_2 < r_1 x_1, x_1 < 0, x_2 < 0, \\ \dfrac{r_1 x_1 - r_2 x_2}{r_1 x_1}, r_2 x_2 \ge r_1 x_1, x_1 < 0, x_2 < 0, \\ 1, x_1 < 0, x_2 \ge 0, \\ 1, x_1 \ge 0, x_2 < 0. \end{cases} \tag{7}$$

for all model operating conditions. A zero wheel slip represents the equality of the wheel and the vehicle velocities, while the slip value equal to one tells us that the tire is not rotating and the wheels are skidding on the road surface, meaning that the vehicle is no more steerable.

The road adhesion coefficient $\mu(\lambda)$ is a nonlinear function of wheel slip and other physical variables, and one of its model can be given by:

$$\mu\left(\lambda\right) = \frac{w_4 \lambda^p}{a + \lambda^p} + w_3\lambda^3 + w_2\lambda^2 + w_1\lambda\,. \tag{8}$$

Equation (6) can be rewritten as:

$$\dot{x}_1 = S(\lambda)(c_{11}x_1 + c_{12}) + c_{13}x_1 + c_{14} + (c_{15}S(\lambda) + c_{16})s_1(x_1)M_1\,,$$
$$\dot{x}_2 = S(\lambda)(c_{21}x_1 + c_{22}) + c_{23}x_1 + c_{24} + c_{25}S(\lambda)s_1(x_1)M_1\,. \tag{9}$$

where:

$$\begin{gathered} S\left(\lambda\right) = \frac{s\mu\left(\lambda\right)}{L\left(\sin\varphi - s\mu\left(\lambda\right)\cos\varphi\right)}, c_{11} = \frac{r_1 d_1}{J_1}, \\ c_{12} = \frac{\left(s_1 M_{10} + M_g\right) r_1}{J_1}, c_{13} = -\frac{d_1}{J_1}, c_{14} = -\frac{s_1 M_{10}}{J_1}, \\ c_{15} = \frac{r_1}{J_1}, c_{16} = -\frac{1}{J_1}, c_{21} = -\frac{r_2 d_1}{J_2}, c_{22} = -\frac{\left(s_1 M_{10} + M_g\right) r_2}{J_2}, \\ c_{23} = -\frac{d_2}{J_2}, c_{24} = -\frac{s_2 M_{20}}{J_2}, c_{25} = -\frac{r_2}{J_2}. \end{gathered} \tag{10}$$

In the braking phase, the wheel speed will be lower than vehicle speed, i.e. $r_2 x_2 \ge r_1 x_1$ and $x_1 > 0$, $x_2 > 0$, so that the wheel slip is determined by:

$$\lambda = \frac{r_2 x_2 - r_1 x_1}{r_2 x_2} \tag{11}$$

In that case, since $s = s_1 = s_2 = 1$, (9) is rewritten as:

$$\begin{aligned} \dot{x}_1 &= S(\lambda)(c_{11}x_1 + c_{12}) + c_{13}x_1 + c_{14} + (c_{15}S(\lambda) + c_{16})M_1, \\ \dot{x}_2 &= S(\lambda)(c_{21}x_1 + c_{22}) + c_{23}x_1 + c_{24} + c_{25}S(\lambda)M_1. \end{aligned} \tag{12}$$

ABS controller is designed to regulate the vehicle slip at the desired value, where the friction force, i.e. road adhesion coefficient, reaches its maximum value. That is why we determine vehicle model with wheel slip as a controlled variable. Differentiating (11) results in:

$$\dot{\lambda} = -\frac{r_1}{r_2 x_2}\dot{x}_1 + \frac{r_1 x_1}{r_2 x_2^2}\dot{x}_2 . \tag{13}$$

Putting (12) in (13) finally yields and taking into account that:

$$\lambda = 1 - \frac{r_1 x_1}{r_2 x_2} \Rightarrow x_1 = \frac{r_2}{r_1}(1-\lambda)x_2 , \tag{14}$$

yields:

$$\dot{\lambda} = f(\lambda, x_2) + g(\lambda, x_2) M_1 ,\ x_2 \neq 0 , \tag{15}$$

where

$$\begin{aligned} f(\lambda, x_2) = &-\left(\begin{array}{l} \left(S(\lambda)c_{11} + c_{13}\right)(1-\lambda) + \\ + \frac{r_1}{r_2 x_2}\left(S(\lambda)c_{12} + c_{14}\right) \end{array} \right) + \\ &+ \frac{(1-\lambda)}{x_2}\left(\begin{array}{l} \left(S(\lambda)c_{21}\frac{r_2}{r_1}(1-\lambda) + c_{23} \right) x_2 + \\ + S(\lambda)c_{22} + c_{24} \end{array} \right) \end{aligned} \tag{16}$$

$$g(\lambda, x_2) = -\frac{r_1}{r_2 x_2}\left(c_{15}S(\lambda) + c_{16} - \frac{r_2}{r_1}c_{25}S(\lambda)(1-\lambda) \right). \tag{17}$$

III. Sliding Mode Control Based on Constant Plus Proportional Reaching Law

Since the system is of first order, the switching function is selected as:

$$\sigma = \lambda - \lambda_r , \tag{18}$$

where λ_r is the constant reference wheel slip. The main control design objective is to find control providing $\sigma = 0$ and consequently $\lambda = \lambda_r$. The switching function dynamics is defined via the constant plus proportional reaching law [3]:

$$\dot{\sigma} = \dot{\lambda} = -M_k\sigma - M_Q \operatorname{sgn}(\sigma), M_k > 0, M_Q > 0 , \tag{19}$$

enabling the finite reaching time determined by:

$$t_r < \ln\left(\left(M_k|\sigma| + M_Q\right)/M_Q\right)/M_k . \tag{20}$$

By substituting (19) in (15), the control torque becomes:

$$M_1 = -g(\lambda, x_2)^{-1}\left(f(\lambda, x_2) + M_k\sigma + M_Q \operatorname{sgn}(\sigma)\right). \tag{21}$$

Since the nominal values of f and g are $\hat{f}$ and $\hat{g}$ respectively, the control torque implemented in real control is:

$$M_1 = -\hat{g}(\lambda, x_2)^{-1}\left(\hat{f}(\lambda, x_2) + M_k\sigma + M_Q \operatorname{sgn}(\sigma)\right). \tag{22}$$

For the sake of simplicity, we denote $g(\lambda, x_2) = g$, $\hat{g}(\lambda, x_2) = \hat{g}$, $f(\lambda, x_2) = f$ and $\hat{f}(\lambda, x_2) = \hat{f}$. We assume that $|\hat{f}| < \hat{F}$, $|f - \hat{f}| < \varepsilon_f$ and $|1 - g/\hat{g}| < \varepsilon_g < 1$, where $\hat{F}$, ε_f and ε_g are the positive real constants, as well as $g/\hat{g} > 0$.

The implementation of (22) in (15) gives:

$$\dot{\sigma} = f - \hat{f} + \hat{f}\left(1 - \frac{g}{\hat{g}}\right) - \frac{g}{\hat{g}}M_k\sigma - \frac{g}{\hat{g}}M_Q \operatorname{sgn}(\sigma). \tag{23}$$

The existance conditions of sliding mode is fulfilled:

$$\sigma\dot{\sigma} = \frac{g}{\hat{g}}\left(\frac{\hat{g}}{g}\left(f - \hat{f}\right)\sigma + \frac{\hat{g}}{g}\hat{f}\left(1 - \frac{g}{\hat{g}}\right)\sigma - M_k\sigma^2 - M_Q|\sigma| \right) < 0 , \tag{24}$$

if M_Q is chosen in accordance with:

$$M_Q > \max\left(\left| \frac{\hat{g}}{g}\left(f - \hat{f}\right) + \frac{\hat{g}}{g}\hat{f}\left(1 - \frac{g}{\hat{g}}\right) \right| \right), \tag{25}$$

which is satisfied if

$$M_Q > \frac{\varepsilon_f + \hat{F}\varepsilon_g}{1 - \varepsilon_g} , \tag{26}$$

since $1 - \varepsilon_g < g/\hat{g} < 1 + \varepsilon_g \Rightarrow 1/(1+\varepsilon_g) < \hat{g}/g < 1/(1-\varepsilon_g)$.

M_k is selected to make the reaching phase as faster as possible.

IV. Experimental Results

For the practical verification of the proposed control method, the ABS produced by Inteco [14] is utilized. The ABS framework is previously described in Section II and it represents the open-architecture software environment for real-time control experiments on the basis of MATLAB and Simulink tools.

Both simulation and real-time experiments are performed and results are given in Figs. 2 and 3. Each figure consists of three subplots representing the responses of wheel and vehicle velocities (speeds), the wheel slip and the control brake torque, respectively. The reference wheel slip is considered to be constant and $\lambda_r = 0.2$.

Firstly, the digital simulation is done. Fig. 2 shows the case with $M_k = 2$ and $M_Q = 1$. The sliding mode exists, but the chattering is not too large since the constant component of reaching law control is taken to be as small as possible. The proportional term, ensuring existence of sliding motion with faster reaching time, enables such selection of M_Q .

Figure 3 presents the experimental results performed in the previous described real-time framework. To cope with unmodelled dynamics, M_k and M_Q are chosen to be 10 and 4, respectively. It can be notice that experimental results are similar to the simulation ones, despite the presence of noise and the fact that the control input is more limited than in the case with digital simulation. The proposed control approach slightly improves the system accuracy in comparison with the results given in [15].

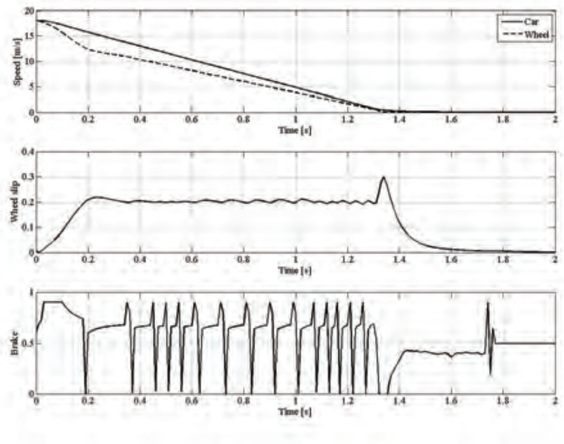

Fig. 2. ABS responses: SMC with constant plus proportional reaching law (simulation results)

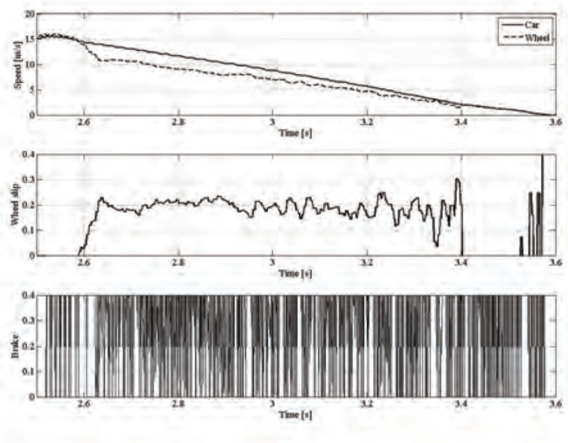

Fig. 3. ABS responses: SMC with constant plus proportional reaching law (experimental results)

V. CONCLUSION

This paper treats the sliding mode control of anti-lock braking system on the basis of constant plus proportional reaching law method. Both digital simulation and experimental results shows good performances in relation to traditional sliding mode control concepts.

ACKNOWLEDGEMENT

This work was supported in part by the Serbian Ministry of Science and Technology within the projects II 43007, II 44006 and TR 35005.

REFERENCES

[1] A. Zanten, R. Erhardt and A. Lutz, "Measurement and Simulation of Transients in Longitudinal and Lateral Tire Forces", SAE Paper, vol. 99, no. 6, pp. 300-318, 1990.

[2] J. Y. Hung, W. Gao and J. C. Hung, "Variable Structure Control: A Survey", IEEE Transactions on Industrial Electronics, vol. 40. no. 1, 1993.

[3] W. Gao and J. C. Hung, "Variable Structure Control of Nonlinear systems: A New Approach", IEEE Transactions on Industrial Electronics, vol. 40, no. 1, 1993.

[4] V. I. Utkin, "Sliding Mode Control Design Principles and Application to Electric Drives", IEEE Transactions on Industrial Electronics, vol. 40, no. 1, 1993.

[5] Y. Oniz, E. Kayacan and O. Kaynak, "Simulated and Experimental Study of Antilock Braking System Using Grey Sliding Mode Control", ISIC. IEEE International Conference on Systems, Man and Cybernetics, pp. 90-95, 7-10 October 2007.

[6] E. Kayacan, Y. Oniz and O. Kaynak, "A Grey System Modeling Approach for Sliding-Mode Control of Antilock Braking Systems", IEEE Transactions on Industrial Electronics, vol. 56, no. 8, pp. 3244-3252, 2009.

[7] N. Hamzah, M.Y. Sam and A. A. Basari, "Enhancement of Driving Safety Feature via Sliding Mode Control Approach", Fourth International Conference on Computational Intelligence, Robotics and Autonomous Systems, pp. 116-120, November 28-30, 2007.

[8] C. Unsal and P. Kachroo, "Sliding Mode Measurement Feedback Control for Antilock Braking Systems", IEEE Transactions on Control Systems Technology, vol. 7, no. 2, pp. 271-281, 1999.

[9] S. Drakunov, U. Ozguner, P. Dix and B. Ashrafi, "ABS Control Using Optimum Search via Sliding Modes", IEEE Transactions on Control Systems Technology, vol. 3, no. 1, pp. 79-85, 1995.

[10] A. El Hadri, J. C Cadiou and N. K. M'sirdi, "Adaptive Sliding Mode Control of Vehicle Traction", 15th Triennial World Congress, July 21-26, 2002.

[11] M. Wu and M. Shih, "Using the Sliding-Mode Pwm Method in an Anti-lock Braking System", Asian Journal of Control, vol. 3, no. 3, pp. 255-261, 2001.

[12] M. Wu and M. Shih, "Simulated and Experimental Study of Hydraulic Anti-lock Braking System Using Sliding-mode PWM Control", Mechatronics, vol. 13, no. 4, pp. 331-351, 2003.

[13] S. Zheng, H. Tang, Z. Han and Y. Zhang, "Controller Design for Vehicle Stability Enhancement", Control Engineering Practice, vol. 14, no. 12, pp. 1413-1421, 2006.

[14] Inteco, "The Laboratory Anti-lock Braking System Controlled from PC"-User's Manual, (2008) available at www.inteco.com.pl.

[15] D. Antić, V. Nikolić, D. Mitić, M. Milojković and S. Perić, "Sliding Mode Control of Anti-lock Braking System: An Overview", Facta Universitatis Series: Automatic Control and Robotics, vol. 9, no. 1, pp. 41-58, 2010.